Nitrogen 1*s* NEXAFS and XPS spectroscopy of NH_3-saturated Si(001)-2×1: Theoretical predictions and experimental observations at 300 K

C. Mathieu, Xuxu Bai,* F. Bournel, J.-J. Gallet, S. Carniato, and F. Rochet†
Laboratoire de Chimie Physique Matière et Rayonnement, Unité Mixte de Recherche CNRS 7614, Université Pierre et Marie Curie, 75231 Paris Cedex, France

F. Sirotti, M. G. Silly, and C. Chauvet
Synchrotron SOLEIL, L'Orme des Merisiers, Saint-Aubin, BP 48, 91192 Gif sur Yvette Cedex, France

D. Krizmancic
Laboratorio Nazionale TASC-INFM, S.S. 14 km 163.5, Area Science Park, 34012 Trieste, Italy

F. Hennies
MAX-Lab, Lund University, P.O. Box 118, 221 00 Lund, Sweden
(Received 24 November 2008; published 21 May 2009)

In the light of hybrid functional density-functional theory calculations of the core-excited and core-ionized states, this paper discusses original N 1*s* x-ray photoemission spectroscopy (XPS) and near-edge x-ray absorption fine-structure (NEXAFS) experimental data on the single-domain (vicinal) Si(001)-2×1 surface saturated by NH_3 at 300 K. The theoretical approach enables to discuss the vibrational shape of the N 1*s* XPS spectrum and quantifies the binding-energy splitting due to intrarow and inter-row hydrogen bondings between amine pairs. The observed N 1*s* NEXAFS peaks are interpreted through the analysis of the contour maps of the antibonding Kohn-Sham orbitals of the NH_2 adsorbate and through the Δ Kohn-Sham calculation of the transition energies, laying a theoretical basis for a discussion of the adsorbate spatial orientation. Finally, suggestions are given for future directions of research to get a further knowledge of a system that has potential applications as a template for molecular layer deposition and supramolecular assembly.

DOI: 10.1103/PhysRevB.79.205317 PACS number(s): 81.05.Cy, 81.07.−b, 82.30.Rs, 82.20.Wt

I. INTRODUCTION

Motivated in the early 1990s by technological considerations related to fabrication processes of microelectronics, that is, silicon nitridation,[1–6] the study of the adsorption and reaction of NH_3 on Si(001)-2×1 is experiencing a renewed interest,[7–16] especially because surface imaging by scanning tunneling microscopy (STM) has pointed to the self-assembly capacity of the adsorbates.[8,10–12,14–16] More generally, the study of adsorption modes of nucleophilic lone-pair bearing molecules, such as ammonia and amines,[17–20] has raised a great interest as these molecules probe the "zwitterionic" nature of the buckled surface dimers that orientates chemical reactions *to first order* [see Ref. 21, where an updated discussion of the (001) surface reconstruction can be found] and as their spatial ordering at the surface is a consequence of interactions mediated through the silicon surface electronic states.[22]

Concerning the adsorption of ammonia on Si(001)-2×1, the consensus is the following: vibrational spectroscopies[1,3,7,13] as well as x-ray photoemission spectroscopy (XPS) (Refs. 4–6 and 9) show that the reaction is dissociative via N-H bond breaking. N 1*s* XPS (Refs. 5 and 9) combined with theoretical calculations[23] indicates that molecular decomposition is limited to the formation of Si-NH_2 and Si-H groups on Si(001). The molecular adsorption state—the molecule donates its lone pair to the electrophilic "down" dimer atom—is a metastable intermediate state observed by STM only in very small amounts at 65 K,[8] in contrast to the case of tertiary amines that can remain blocked in this state at 300 K.[17–20]

On the other hand, there is general consensus neither on the adsorption sites of the molecular fragments nor on the relative distribution of the various possible adsorption patterns. Indeed NH_2 and H can be attached either to the *same* dimer ("on-dimer" configuration) or to two adjacent dimers pertaining to the same row ("interdimer" configuration). On-dimer dissociation leads to a nitrogen saturation coverage of 0.5 monolayer (ML), that is, one molecule per dimer, a value compatible with ammonia uptake measurements[2] (0.50 ± 0.15 ML). Recent STM images published by Owen *et al.*[10] and Bowler and Owen[11] are interpreted in terms of "on-dimer" NH_2 and H adducts displaying different contrasts (NH_2 is "brighter" than H for a −2 V sample bias): NH_2 groups would align on the same side of a dimer row (linear mode) or on alternating sides (zigzag mode) (see Fig. 1) with a statistical ratio linear:zigzag close to 1:1 for adsorption at 300 K.[10] However, Chung *et al.*[12,14,16] challenged the preceding interpretation of linear patterns: they are reinterpreted as resulting from "interdimer" reactions, with H and NH_2 fragments on the same side of the row and silicon dangling bonds on the opposite side. The work by Chung *et al.*[12,14] pointed also to a large dominance of zigzag patterns at 300 K at high coverage, in contrast to Refs. 10 and 11.

Neither is there any agreement from infrared studies on the relative distribution of the zigzag and linear patterns. The infrared studies are based on the sensitivity of the Si-H stretching frequency toward H bond formation between ad-

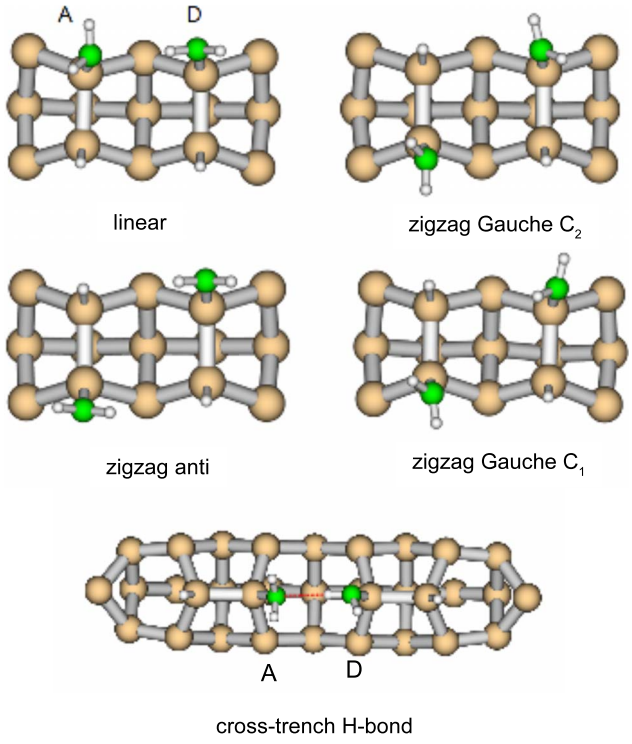

FIG. 1. (Color online) The adsorption patterns of ammonia on Si(001)-2×1 assuming the on-dimer dissociation process. The ball and stick picture is the result of a DFT quantum chemistry calculation (see text), using two-dimer clusters to mimic the surface, the "intrarow" $Si_{15}H_{16}$ cluster and the "cross-trench" $Si_{33}H_{30}$ cluster. H, N, and Si atoms are represented by small white, medium size green, and large brown spheres, respectively (the H atoms used to passivate the cluster dangling bonds are not represented). The following nomenclature is used: *A* (H-acceptor), *D* (H-donor).

jacent NH_2 in on-dimer linear patterns. An earlier study was indicative of a zigzag absorption mode,[7] while a recent work[13] points to a majority of "linear patterns" (linear:zigzag=2:1). As shown in the theoretical work by Rignanese and Pasquarello,[24] N 1*s* XPS would be able to detect directly the formation of hydrogen bonds in amine pairs placed on the *same side of the dimer row.* By performing a periodic density-functional theory (DFT) calculation, within the "pure" generalized gradient approximation (GGA), Rignanese and Pasquarello found that for a nitrogen-nitrogen distance of 3.42 Å, the H donor and H acceptor nitrogen 1*s* binding energies are split by 0.4 eV. The H acceptor nitrogen has the highest binding energy. The sizable impact of a relatively weak H bonding on core-level binding energies has been further confirmed by a recent hybrid DFT [Becke 3-parameters Lee-Yang-Parr (B3LYP) exchange-correlation functional] quantum chemistry work by our group on a similar system, water-dosed Si(001)-2×1 that exhibits Si-H and Si-OH moieties.[25] The O 1*s* binding energy is split by 0.28 eV between paired H-acceptor/H-donor hydroxyls, with an O-O distance of 3.373 Å (close to the N-N distance calculated in Ref. 24). In fact, as no doublet was observed in the already published experimental N 1*s* XPS spectra of the ammonia-dosed surface,[5] Rignanese and Pasquarello[24] concluded that DFT calculations lend little support to the "linear pattern." In addition to the intrarow interaction considered in Ref. 24, we examine the formation of H-bond between two adjacent NH_2 pertaining to two different dimer rows. Our calculations (Sec. IV A) will show that this "cross-trench H-bond" (see Fig. 1) is even stronger than the intrarow one.

Angular- and energy-dependent N 1*s* photoelectron diffraction (PED) measurements combined with multiple-scattering calculations can provide valuable information on the adsorbate geometry. In the PED work by Franco *et al.*,[26] Si-N distances and bond angle are deduced from the experimental data fitted with the isolated (i.e., not H bonded) amine model. To what extent amine pairing in adjacent sites (within and across dimer rows) has an influence on the PED curves remains an open question.

Adsorbate patterning in the Si(001)-2×1:NH_3 system is determined by a subtle balance between two possible mechanisms: (i) the interaction can be mediated by the substrate and (ii) the interaction can be direct through H bonding (between neighboring NH_2 or between NH_2 and an incoming NH_3 molecule). As Widjaja and Musgrave showed it theoretically,[22] the poisoning of the site adjacent to that of molecular adsorption favors zigzag patterns if the molecular precursor lifetime is sufficiently long; on the other hand, $SiNH_2$-NH_3 interactions via H bond formation (reinforced by charge transfer via the substrate) favor linear patterns. However, the interaction is not limited to dimer rows: in Ref. 11, Bowler and Owen proposed that H bonding between an incoming NH_3 and an existing NH_2 group could also lead to correlated adsorption across dimer rows. A correlation analysis of STM images of the surface at very low coverage first presented by Chung *et al.*[14] and then reinterpreted by Owen and Bowler[15] supports this view. Judging from the occupied-state state image of the surface at high coverage given in Fig. 2 of Ref. 11 and admitting that the bright spots correspond to amines, about 20% of the NH_2 groups are in a position to form cross-trench H bonds.

A better knowledge and control of ammonia adsorption patterns is indeed crucial, as the NH_2 covered Si(001) surface could be exploited to graft arrays of multifunctional molecules of technological interest without incurring the risk of producing multiple adsorption geometries, which is often observed when these molecule interact directly with the clean surface.[27,28] While the "classical" reaction schemes of amines with organic functionalities have not been tested yet,[29] it has been proven that an organometallic molecule tetrakis(dimethylamido)titanium reacts at 300 K with $SiNH_2$ groups in UHV conditions.[30] In the field of supramolecular assembly, it has been reported that amine fragments on Si(001) govern the crystalline growth of a molecular solid copper phthalocyanine via the repulsion between the π system of the deposited molecule and the amine lone pair.[31] These two very recent observations will certainly fuel the interest for studying and controlling the adsorption patterns of NH_3-reacted Si(001).

Despite the numerous photoemission studies devoted to ammonia-reacted Si(001),[4–6,9,26] a further characterization of its electronic structure was worth being undertaken, especially in view of the questions related to surface patterning. The present work presents high-energy resolution

(~80 meV) XPS and original near-edge x-ray absorption fine-structure (NEXAFS) spectroscopy[32] data. NEXAFS, which was still lacking to the ensemble of spectroscopies applied to the present system, probes the empty states of *p* symmetry localized around the core-excited nitrogen. In this respect, NEXAFS is complementary to the valence-band photoemission that probes occupied states, however, with the drawback of mixing adsorbate and substrate contributions. Using linearly polarized radiation and carrying out angle-dependent measurements of the absorption intensity, NEXAFS gives information on the spatial orientation of the unoccupied molecular orbitals (UMOs).[32] The XPS and NEXAFS experimental data were interpreted in the light of a hybrid functional DFT calculation of adsorption geometries and core-ionized/core-excited states. Given the present experimental resolution, a special attention was devoted to the simulation of the XPS N 1*s* spectrum, including vibrational broadening and H-bond induced binding-energy shifts. The calculation of the NEXAFS N 1*s* transition energies has enabled an unambiguous attribution of the main experimental spectral features to a set of unoccupied antibonding orbitals. Finally, the NEXAFS spectra (in the framework of the dipolar approximation) have been computed for various adsorption patterns and their theoretical dichroic behavior compared with the experimental one.

II. EXPERIMENT

A. Setup and sample preparation

The experiments have been performed at TEMPO beamline[33] SOLEIL synchrotron facility (Saint Aubin, France). The radiation source is an Apple II type insertion devices (HU80). The photon energy selection is obtained by simply rotating "variable line spacing" plane gratings. The resolving power $E/\Delta E$ is better than 15000 on the whole energy range (50–1500 eV). 90% of the photon intensity is focused in a spot 45 μm long in the horizontal direction and 5–10 μm wide in the vertical dimension using two mirrors in a Wolter configuration (a spherical mirror is directly followed by a toroidal mirror and the photon beam is deviated horizontally).

The beamline is equipped with an end station dedicated to electron spectroscopy studies of surfaces. The analysis chamber (base pressure$=10^{-10}$ mbar) is equipped with a SCIENTA-200 electron analyzer, fitted with a new delay-line two-dimensional (2D) detector, designed and commercialized by the Instrumentation and Detectors Laboratory of ELETTRA Synchrotron Facility (Trieste, Italy). A UHV preparation chamber fitted with a heating stage is connected to the analysis chamber.

To take a full advantage of the capability of N 1*s* NEXAFS spectroscopy to determine NH_2 bond orientations, the ammonia molecule needs to be deposited on a single-domain vicinal surface. It is well known that on-axis nominal (001) surfaces consist of 2×1 and 1×2 domains in equal quantities, with the dimer rows of one domain running perpendicular to the dimer rows of the other. On the other hand, a vicinal Si(001) surface cut by 5° off [001] axis toward $[1\bar{1}0]$ forms a regular array of bisteps (of height 2.715 Å) and single 2×1 reconstructed surface domain terraces (of an average width 31.03 Å). Bistep formation implies that all dimer rows are perpendicular to the step edge; with a 5° miscut angle, dimer rows on terraces contain on the average 7.6 Si_2 units[34] plus—on the step edge—a pair of trigonally rebonded atoms.[35] The (phosphorus) *n*-doped (resistivity 5 $\Omega\times$cm) wafers were submitted to a prolonged outgassing at 600 °C in the UHV preparation chamber. Then the samples were transferred in the analysis chamber and cleaned of their silica protective layer by heating at ~1100 °C. The surface cleanliness was checked by XPS. The silicon surface was then saturated by NH_3 reaction products by dosing *at room temperature* under a pressure of 10^{-7} mbar (ion gauge uncorrected reading) for 15 min. We have checked by low-energy electron diffraction (LEED) that a single-domain pattern is observed. We give in Fig. 2 the LEED image of a vicinal surface saturated with ammonia. Note that half-order spots are only seen along the [110] direction. Spot doubling along the $[1\bar{1}0]$ direction reflects the step edge periodicity of terraces with equal widths.

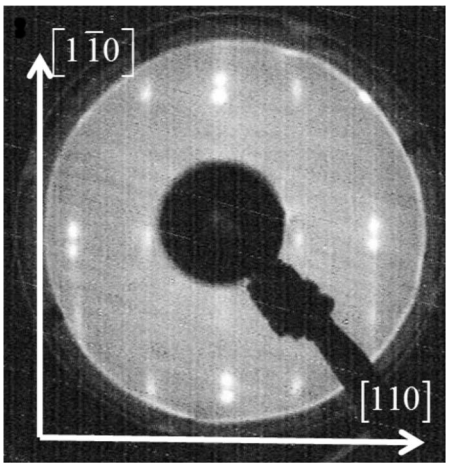

FIG. 2. LEED pattern of a Si(001)-2×1 vicinal surface saturated with ammonia at room temperature. Bistep edges and dimer axes are along the [110] direction (the miscut is along $[1\bar{1}0]$). Note the absence of half-order spots along $[1\bar{1}0]$, the dimer row direction. The energy of the electron beam is 56.5 eV.

B. XPS

The Si 2*p* core-level spectra were measured at $h\nu=130$ eV (overall experimental resolution ~30 meV). The N 1*s* core-level spectra were recorded at $h\nu=455$ eV (overall experimental resolution ~80 meV). Electrons were detected at 0° from the sample surface normal and at 46° from the polarization vector **E**. The zero binding energy (the Fermi level) is taken at the leading edge of a clean metal surface in electrical contact with the silicon crystal. The binding energy of the Si $2p_{3/2}$ component of the clean (*n*-doped) silicon surface is found at 99.30 eV.

C. N KVV Auger yield NEXAFS measurement and data analysis

The x-ray absorption spectra were measured in the so-called Auger yield mode, exploiting the 2D detection of the

electron analyzer, operated in the so-called "fixed mode." The pass energy was set to 200 V, so that the nitrogen KVV Auger yield could be measured within an energy window of ~12 eV centered at a kinetic energy of 375 eV. The photon energy was scanned in the 395–420 eV range. As the surface nitrogen coverage is low (~0.5 ML), a photon bandwidth of 80 meV was chosen to obtain good Auger yield statistics within reasonable acquisition times (typically 30 min).

The raw N KVV Auger yield spectra from the ammonia-reacted sample were divided by the reference grid current that monitors the x-ray intensity variation with $h\nu$. To avoid strong variations in photon intensity versus photon energy due to the undulator peak, the synchronous scanning of undulator gap and monochromator was made. The photon flux increased smoothly by only 30% between $h\nu$=395 eV and $h\nu$=420 eV. This ensured a very reliable normalization procedure, which consists in plotting curves having an equal absorption jump, just before the edge (395 eV) and ~30 eV after.

Finally, the photon energy was calibrated by subtracting the kinetic energy of Si 2*p* photoelectrons excited by first-order radiation ($h\nu$) to that of Si 2*p* photoelectrons excited by the second-order radiation ($2\times h\nu$). To check for synchrotron-radiation damage beam effects, we compared systematically the shape of the N 1*s* XPS spectra before and after the x-ray absorption measurements.

The vicinal surface we used enabled NEXAFS measurements with the electric field vector **E** of the radiation placed at 20° from the surface normal within the $(1\bar{1}0)$ plane (grazing incidence) and placed in the surface plane (normal incidence). For the in-plane geometry, **E** was positioned either orthogonal (along [110]) or parallel to the dimer rows (along $[1\bar{1}0]$), by rotating azimuthally the sample by 90°.

III. COMPUTATIONAL

A. Adsorption geometries

We have started from the isolated amines using a one-dimer cluster (Si_9H_{12}). Ignoring inter-row interactions, zigzag and aligned (intrarow H-bonded) patterns have been reproduced, using a two-dimer-in-a-row cluster ($Si_{15}H_{16}$). A cross-trench two-dimer cluster ($Si_{33}H_{30}$) has been used to examine the H-bond interaction between two amines pertaining to two adjacent dimer rows. The competition between intrarow and inter-row hydrogen bondings that need still larger silicon clusters has not been examined.

Electronic structure calculations were completed with the GAMESS(U.S.) (Ref. 36) software package using Becke three parameter exchange functional,[37] along with the Lee-Yang-Parr[38] gradient-corrected correlation functional (the so-called B3LYP functional). We have used effective core potentials [due to Stevens, Basch, Krauss, and Jasien (SBJK) and built into the GAMESS package] for Si atoms, a 6-31G* basis set for the terminating H atoms of the clusters, a 6-31G* *plus* three diffuse functions (one *s* and two *p*) for the H atoms of the adsorbate, and a 6-311G* basis set (plus two diffuse functions, one *s* and one *p*) for N. The added diffuse functions enable a better theoretical treatment of the hydrogen bond, as we have verified in the case of the water dimer $[(H_2O)_2]$.[25] Besides the basis set choice, it is generally admitted that the hybrid approach gives better results than the pure GGA method in the calculation of H bonds, the latter tending to overestimate the bond strength.[39,40] During the computation all silicon clusters were fully relaxed, except the $Si_{33}H_{30}$ cluster for which the four Si atoms at the bottom were kept at bulk lattice positions. The calculated adsorption geometries are shown in Fig. 1, while characteristic distances and angles are collected in Table I.

For all models, the Si-N distance (1.75–1.77 Å) we find is consistent with the bond length deduced from the PED study,[26] that is, 1.73 ± 0.08 Å. We calculate a Si-N bond angle relative to the surface normal of 21.2° for the gauche models in excellent accord with the PED value of $21°\pm4°$. The angle we find for the "antimodel" (28.8°) is only 4° off the interval of values given by PED. For the (intrarow) linear pattern, we calculate an N-N distance (a H-bond length) of 3.55 Å, significantly shorter than the lattice spacing of 3.84 Å along the $[1\bar{1}0]$ direction. This demonstrates the formation of a hydrogen bond (length 2.69 Å) between the two amine groups. The N-N distance we find is longer (by ~4%) than those calculated with a pure GGA functional, i.e., 3.44 Å in the work of Bowler and Owen[11] and 3.42 Å in the work of Rignanese and Pasquarello.[24] The comparison to the above-mentioned periodic slab calculation also indicates that the (fully relaxed) cluster is not so "floppy" as to lead to unrealistic short distances. For its part, the cross-trench H-bonded NH_2 pair model ($Si_{33}H_{30}$ cluster) gives a N-N bond distance (H-bond length) of 3.30 Å (2.27 Å) significantly smaller than that of the intrarow interaction.

Only optimized geometry energies calculated with the same cluster size, that is, the two-dimer intrarow cluster $Si_{15}H_{16}$, can be consistently compared. They are also reported in Table I referenced to the linear model energy, that is, the most stable structure. The three zigzag geometries have systematically higher energies than the linear pattern by 0.050–0.070 eV (1.2–1.5 kcal/mol). This calculated energy difference agrees with the previous quantum chemistry B3LYP calculation by Queeney *et al.*[7] (1 kcal/mol) but is larger than that found by Rignanese and Pasquarello;[24] 0.5 kcal/mol (0.02 eV) per 2×2 surface unit (a value that is within the accuracy of their method) with a GGA functional. The energy difference of +14 meV (0.3 kcal/mol) we find between the zigzag gauche-C_2 and the zigzag anti (Fig. 1 and Table I) that lies within the accuracy range of our calculation is notably smaller than the value of 40 meV per 2×2 surface unit given in Ref. 41.

B. Core-excited and core-ionized calculations

The Franck-Condon (FC) principle states that during an electronic transition the molecular geometry can be assumed to be unchanged. Within this framework, the ground-state optimized geometries we find following the procedure described in Sec. III A for the molecule plus Si cluster system is the starting point of the calculation of ionization potentials (IPs) and NEXAFS transition energies. The quantum chemical *ab initio* calculations of the N 1*s* excited states are also

TABLE I. Calculated bond lengths *d*, N-N distances (in Å), bond angles, and dihedral angles (in degree) obtained from the geometry optimizations shown in Fig. 1. B3LYP hybrid functional, "large basis" sets (see Sec. III C) were used. Results of GGA periodic calculations by Rignanese and Pasquarello (Ref. 24) and Bowler and Owen (Ref. 11) are given for comparison. For the H-donor group, (*) indicates the free hydrogen, while (†) indicates the atom involved in the H bond. For calculations using the double-dimer $Si_{15}H_{16}$ clusters, optimized structure energies (in meV) are referenced to that of the most stable one: the linear pattern.

Pattern		Optimized structure energy	$d_{Si\text{-}N}$	$d_{N\text{-}H}$	$d_{Si\text{-}H}$	$d_{H\ bond}$	NN	∠Si-Si-N
Linear	$Si_{15}H_{16}$	0				2.69,2.61[a]	3.55,3.42,[b]3.44[a]	
acceptor			1.75(1.76)	1.013	1.50			
donor			1.75(1.79)	$1.011^{*}/1.015^{\dagger}$	1.50			
Zigzag (anti)	$Si_{15}H_{16}$	+52	1.75(1.76)	1.011	1.50		5.70	118.8
Zigzag (gauche-C_2)	$Si_{15}H_{16}$	+66	1.75	1.011	1.49		5.21	111.2
Zigzag (gauche-C_1)	$Si_{15}H_{16}$	+50	1.75	1.012	1.49	4.79	5.41	111.2
Cross trench	$Si_{15}H_{16}$				1.51	2.27	3.30	
acceptor			1.75	1.014	1.51			120.9
donor			1.75	$1.017^{*}/1.022^{\dagger}$	1.51			112.25

[a]Reference 11.
[b]Reference 24.

performed at a DFT level of theory.[42,43] We used a modified version of the GAMESS(U.S.) program, enabling (i) the choice of a fractional occupancy for the core hole and (ii) the calculation of singlet core excited energy values.[44]

The excited atom was described with a large basis set. For N we use the IGLOO-III basis, to which diffuse functions were added. For the H atoms, passivating the silicon cluster a 6-31G* basis was used; for those of the adsorbate, diffuse functions were added. For the calculation of N 1*s* IP (the so-called *vertical transition energy*), the ΔKohn-Sham method (denoted hereafter ΔKS) is applied. The IP is the difference between the energy of the excited state represented by a core hole in the 1*s* orbital and that of the ground state. Absolute values of NEXAFS transitions are also calculated via the ΔKS procedure. The energy of the core-excited state is obtained by removing one electron from the 1*s* and adding one to the UMO of interest, i.e., by calculating the NEXAFS state $(1s)^1(\mathrm{UMO})^1$. Then the transition energy is obtained as the difference between the energy of the excited state and that of the ground state. The relativistic correction of 0.3 eV is included, according to Triguero.[45] The ΔKS triplet final-state transition energies are corrected using the sum method of Ziegler *et al.*[46] to account for the spin conservation in dipolar transitions leading to a singlet final state. ΔKS energies have been calculated for the molecular orbitals leading to the major oscillator strengths (computed in the framework of the dipolar approximation). A comparison between the ΔKS calculation outputs can be made for the various adsorption models we have considered.

While this separate state Kohn-Sham scheme is a convenient and accurate option for IP and first core-excited transition energies calculations, it is not always applicable to calculate the whole x-ray absorption spectrum due to problems of collapse in optimizing higher-excited states. To circumvent this difficulty, we diagonalize a potential built from orbitals where a 1*s* electron is removed (the full core hole is denoted FCH) and put into one UMO or "distributed" into more UMOs—in the latter case, their occupancy is fractional. The excited electronic levels are then determined by the electrostatic field of the remaining molecular system. The eigenvalues and eigenvectors give the full spectrum of excitation energies and moments. The transition energy is simply the difference between the energy of the virtual orbital and that of the 1*s* orbital and the oscillator strengths are obtained from the eigenvectors within the dipolar approximation.

An *ad hoc* FCH-UMOs potential is found (i) when the relative difference between the various energies corresponds to the calculated ΔKS ones and (ii) when the oscillator strengths (dipolar approximation) compare to those of the ΔKS method. As the absolute values of the energies may be 0.5–1 eV off the ΔKS (and experimental) ones, the NEXAFS spectra are repositioned on an absolute energy scale provided by the energy of the first bound excited state calculated with the ΔKS method described here above. Below the calculated IP, the NEXAFS spectrum consists of the discrete lines calculated by method broadened by convolution with a Gaussian of 0.8 eV full width at half maximum (FWHM). For transitions calculated above IP, we convert the discrete lines into a continuum using the Stieltjes imaging procedure[47] (the calculated continuum cross section is convoluted with the same Gaussian function used for the discrete part below IP).

C. Vibrational fine structure of N 1*s* XPS spectra and its calculation

The theoretical analysis is based on the determination of the energy surface of the ground and the core-ionized states. To estimate the respective contributions of the $Si\text{-}NH_2$ moi-

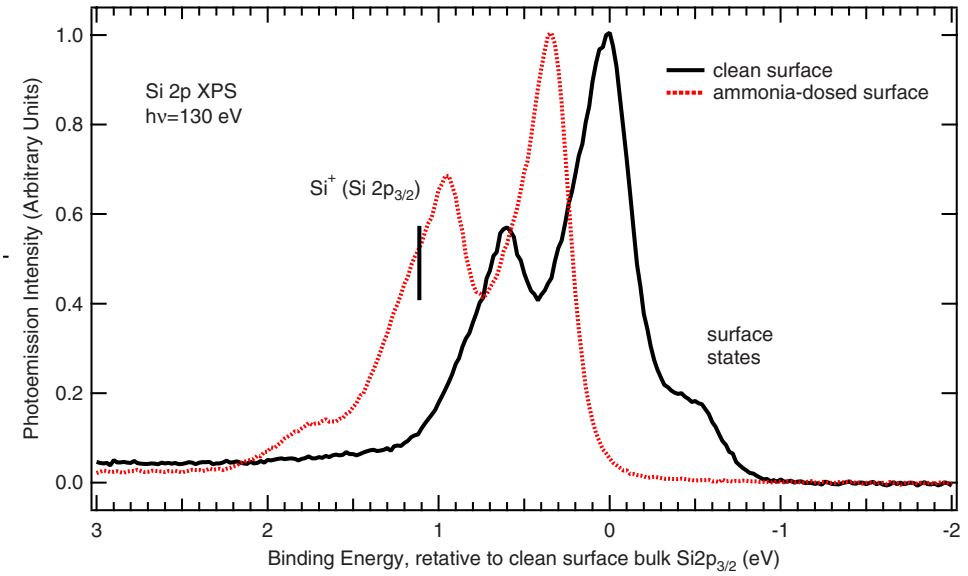

FIG. 3. (Color online) XPS Si $2p$ spectra of the clean surface (solid line) and of the reacted surface (dotted line) after exposure to ammonia under a pressure of 10^{-7} mbar for 15 min (300 K). The photon energy was 130 eV. The bulk line Si $2p_{3/2}$ binding energy of the clean surface (99.30 eV from E_F) is taken as reference energy. Note the complete quenching of the surface states and the associated downward band bending (330 meV); the growth of the Si^+ state (at +0.78 eV from the bulk line of the ammonia-reacted surface).

ety and of the underlying silicon substrate to the vibrational broadening, we have calculated the equilibrium geometries and vibrational frequencies[48] of three models NH_2-SiH_3, NH_2-Si-$(SiH_3)_3$, and H_2N-Si_9H_{12} characterized by an increasing size in the silicon cluster that approximates the substrate. A detailed Franck-Condon analysis of the spectra, as developed in Ref. 49, has been carried out. The vibrational wave function for the core-excited state is assumed to be a product of $3N$-6 one-dimensional harmonic oscillators (where N is the number of nuclei) that are described either by the same or different normal coordinates and sets of frequencies as those of the ground state. The analytical approach is based on the expression of the overlap between two products of harmonic oscillators, where the full core-ionized potential-energy surface is displaced from the ground-state equilibrium position. In order to speed up the calculation, the 6-31G* basis set optimized by Carniato and Millié[50] and Carniato and Luo[51] (referred hereafter as "small bases") has been used.

IV. RESULTS AND DISCUSSION

A. X-ray photoemission

The Si $2p$ XPS core levels measured in surface sensitive conditions at a photon energy of 130 eV (Ref. 52) are shown in Fig. 3. Reaction with ammonia (300 K, 10^{-7} mbar, and 15 min) induces a sizable downward band bending: the bulk Si $2p_{3/2}$ binding-energy shifts from 99.30 eV (clean surface) to 99.63 (eV) (ammonia-dosed surface). The disappearance of the outer-dimer-atom component (at −0.50 eV from the bulk Si $2p_{3/2}$ component of the clean surface) indicates that the surface is saturated. As the coverage is close to one NH_2 per dimer (saturation), all the necessary conditions are gathered to observe possible effects of hydrogen pairing in linear adsorption patterns on N $1s$ XPS and NEXAFS spectra.

The N $1s$ core level of the saturated surface we have measured at $h\nu$=455 eV is given in Fig. 4. The peak can be fitted by a single Voigt component peaked at a binding energy of 398.95 eV. This binding energy is characteristic of Si-NH_2 fragments.[5,9,23] We do not detect $NH_{x(x<2)}$ species that should be found at lower binding energies (from −0.6 to −1.3 eV according to the degree of dehydrogenation[23]). This indicates that the molecular dissociation on a vicinal surface—that besides terrace dimers, presents bistep edge sites (pairs of trigonally bonded silicons) amounting to 11.6% of all the reaction sites of the vicinal surface—is not different from the one observed on a nominal surface.

The overall width of the N $1s$ Voigt profile is 0.675 eV (we take a Lorentzian lifetime width of 115 meV, as for N_2,[53] and a Gaussian width of 600 meV). Despite the experimental resolution (80 meV), we do not observe vibrational series in this symmetric N $1s$ peak. The N $1s$ peak is narrower than those previously measured (0.75 eV[9]) on the Si(001) surface. Considering the instrumental resolution of 80 meV, a Gaussian inhomogeneous broadening (encompassing structural plus vibrational contributions) of 595 meV is deduced. The sources of inhomogeneous broadening are of two types: (i) vibrational and (ii) structural.

Let us first examine the vibrational aspect. As a first step, we have calculated how vibrations could contribute to the N $1s$ XPS spectrum breadth of an *isolated amine*, following the procedure described in Sec. III C. In the core-ionized state, the molecular fragment changes its geometry. For all three models [H_2N-SiH_3, H_2N-$Si(SiH_3)_3$, and H_2N-Si_9H_{12}; see Table II], we note (i) a depyramidalization of the Si-NH_2 unit (the four atoms become coplanar), (ii) a N-H bond-length reduction of 3.7% (0.973 Å instead of ~1.01 Å in the ground state), and (iii) a *strong increase* (9%) in the Si-N bond length [~1.91 Å instead of ~1.75 Å in the ground state for H_2N-$Si(SiH_3)_3$, and H_2N-Si_9H_{12} models]. Changes in frequencies upon core ionization are reported in Table III. The remarkable fact is the strong decrease in ν(Si-N) frequency (from 822 to 531 cm^{-1} for the H_2N-Si_9H_{12} cluster) associated with the elongation of the bond. The FC factors are calculated taking into account the different sets of vibrational frequencies for the core-ionized and ground state. The values of the FC factors indicate that the N $1s$ XPS vibrational profile is determined by the simultaneous excitation of ν(Si-N) and of (high-frequency) ν(N-H) stretching modes,

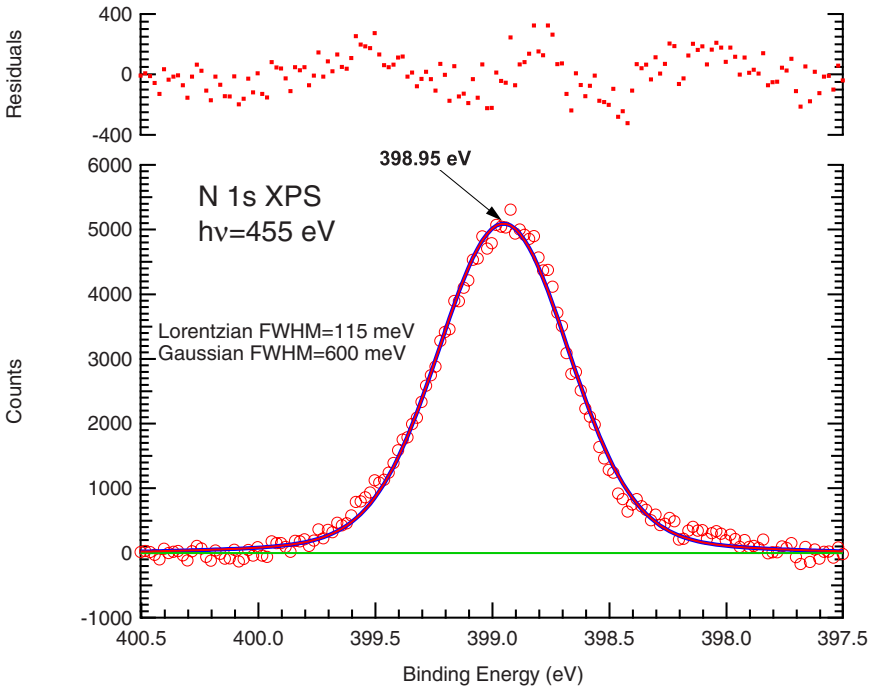

FIG. 4. (Color online) Experimental N 1*s* XPS spectrum (circles) of the NH_3-saturated surface (300 K, 10^{-7} mbar, and 15 min). After Shirley background subtraction, the spectrum is fitted by a single Voigt component at 398.95 eV of FWHM 0.675 eV. The Lorentzian (Gaussian) FWHM is 115 meV (600 meV).

on one hand, and of the Si-$(H)_3$ or Si-$(Si)_3$ symmetric bending modes, on the other hand.

The calculated N 1*s* XPS profiles (including the natural lifetime and the experimental broadening) are reported in Fig. 5 for the three models. Note in passing that the IP (vertical transition; see Table IV) decreases with an increasing number of silicon atoms simulating the substrate.[54] The N 1*s* XPS spectra are in fact composed of many overlapping vibrational progressions, one progression from each excited core-hole state vibrational level in each normal mode. One sees that the spectral shapes are strongly affected by the values of the Si-$(H)_3$/Si-$(Si)_3$ bending mode frequencies (the "substrate contribution"). For the small NH_2-SiH_3 cluster, the FC factors associated to the symmetric bending of the Si-$(H)_3$ moiety are equally distributed over several vibrational overtones (up to $v'=4$). Therefore, the calculated spectrum is rather symmetric, with a FWHM of ~650 meV. In contrast to the preceding, the low frequencies of the Si-$(Si)_3$ bending modes associated to NH_2-Si-$(SiH_3)_3$ and H_2N-Si_9H_{12} clusters lead to FC factors with high values only at the $v=0 \rightarrow v'=0$ transition. Moreover, the fact that the Si-N bond becomes longer and softer in the excited state makes the ν(Si-N) mode reach a high FC only for the $v=0 \rightarrow v'=0$ transition. The conjugation of these two effects leads to *narrow* and *asymmetric* N 1*s* peaks. For the H_2N-Si_9H_{12} cluster, the FWHM is ~320 meV and the high-frequency ν(N-H) series becomes discernible, which—we recall—is not observed experimentally. The conclusion of the present vibrational analysis of the N 1*s* XPS peak, using the "most realistic" cluster (H_2N-Si-Si_9H_{12}), is that an isolated amine cannot provide a sufficiently large vibrational broadening to explain the experimental FWHM of 675 meV. If one assumes (i) that the amines on the real surface can be described as a collection of (nearly) isolated fragments, whose N 1*s* fine vibrational substructure is well described by the preceding approach and (ii) that, for reasons that will be explained further on, their N 1*s* binding energies follow a Gaussian distribution then one finds that this "structural broadening" would have a FWHM of ~0.6 eV (we subtract quadratically the calculated isolated amine N 1*s* peak to the experimental one). While all amines are, at first sight, chemically equivalent, what are the possible causes leading to such a large structural broadening?

Rignanese and Pasquarello[24] already drew attention to the fact that hydrogen bonding between adjacent pairs in (intrarow) linear patterns may have a sizable impact on the N 1*s* binding energies. Using a two-dimer cluster ($Si_{15}H_{16}$), we calculate that the H-acceptor and H-donor nitrogen IPs of the *linear model* are split by 0.4 eV (see Table IV). These two IP values bracket the "noninteracting $SiNH_2$" IP value of the zigzag models. Our B3LYP results are qualitatively and quantitatively in very close agreement with the previous pure GGA calculation. For the cross-trench H-bonded amines (a configuration that was not addressed in Ref. 24), the calculated energy splitting between acceptor and donor IPs is

TABLE II. Calculated bond lengths (in Å), bond angles, and dihedral angles (in degree) of the core-ionized amine (B3LYP hybrid functional and "small" bases, see Sec. III C). A comparison is made with the ground state. Three models are considered.

	Ground state	Core-ionized
Optimized geometry		
∠SiNHH	141.8,[a]141.8,[b]145.5[c]	179,[a]175,[b]180[c]
$d_{Si\text{-}N}$	1.737,[a]1.757,[b] 1.750[c]	1.842,[a]1.917,[b]1.912[c]
$d_{N\text{-}H}$	1.012, 1.013[b,c]	0.976,[a] 0.973[b,c]

[a]H_2N-SiH_3.
[b]H_2N-Si-$(SiH_3)_3$.
[c]H_2N-Si_9H_{12}.

TABLE III. Initial and final-state frequencies (cm^{-1}) calculated for the three clusters H_2N-SiH_3, H_2N-Si-$(SiH_3)_3$, and H_2N-Si_9H_{12}. Franck-Condon (FC) factors are given for v' ranging from 0 to 6. 1000 cm^{-1} which corresponds to 0.12399 eV.

Cluster type	Mode	Initial state Frequency (cm^{-1})	Final State frequency (cm^{-1})	FC factors						
				0	1	2	3	4	5	6
H_2N-SiH_3	Si-$(H)_3$ symmetric bending	1010	960	0.15	0.24	0.26	0.18	0.10	0.04	0.02
	ν(Si-N)	832	626	0.47	0.39	0.12	0.02			
	$\nu(NH_2)$ symmetric stretching	3683	3813	0.62	0.26	0.08	0.03			
H_2N-Si-$(SiH)_3$	Si-$(Si)_3$ symmetric Bending	114	124	0.49	0.11	0.08	0.08	0.08	0.06	0.04
	ν(Si-N)	806	525	0.42	0.22	0.18	0.11	0.05		
	$\nu(NH_2)$ symmetric Stretching	3556	3836	0.80	0.15	0.03				
H_2N-Si_9H_{12}	Si-$(Si)_3$ symmetric Bending	224	221	0.33	0.35	0.21	0.08	0.03		
	ν(Si-N)	822	531	0.48	0.18	0.17	0.11	0.04		
	$\nu(NH_2)$ symmetric stretching	3547	3827	0.59	0.26	0.11	0.02			

0.7 eV. This sizable increase in the IP splitting with respect to the intrarow linear pattern is a consequence of the reduced H-bond length (−0.42 Å).

As stated before, the theoretical vibrational contribution alone (Fig. 5) does not account for the experimental breadth of the N 1*s* peak (675 meV). Let us now examine if H bonding can explain the observed broadening. In Fig. 6, we simulate the N 1*s* peak considering pure isolated amines [Fig. 6(a)], pure (intrarow) linear patterns [Fig. 6(b)], a 50:50 mixture of isolated amine and linear pattern [Fig. 6(c)] (a zigzag:linear ratio close to one at 300 K is suggested by the authors of Refs. 10 and 11), and finally a 40:40:20 mixture of isolated amine, intrarow linear, and cross-trench configurations. Each individual component is a Gaussian of FWHM 0.32 eV, accounting for vibrational,[55] lifetime, and experimental broadening. Looking at Fig. 6(b), it appears that the hypothesis of a pure linear pattern must be eliminated, as the two (0.4 eV apart) components remain well separated in the synthetic curve (this was also the main conclusion of Ref. 24). On the other hand, *mixed patterns* lead to a substantial broadening of the synthetic curve, especially when cross-trench H bonds are taken into account [see curve (d)]. The

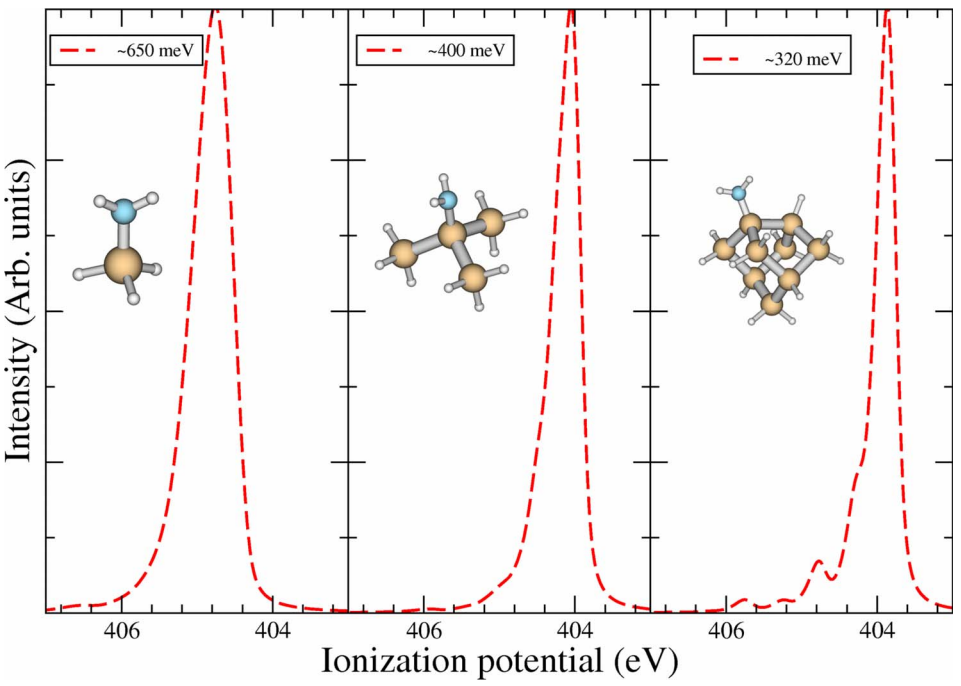

FIG. 5. (Color online) Theoretical vibrational N 1*s* spectra calculated for the three cluster models NH_2-SiH_3, NH_2-Si-$(SiH_3)_3$, and H_2N-Si_9H_{12}. The spectral shape includes the experimental Gaussian broadening and the natural core-hole lifetime. The corresponding FC factors and IP are given in Table III and Table IV, respectively.

TABLE IV. ΔKS calculation of IP and NEXAFS transitions for the isolated Si-NH_2 fragment and the Si-NH_2 pairs in "zigzag anti" and "H-bonded linear" patterns. Energies are given in eV. Large basis sets (see Sec. III B) are used, unless marked by an asterisk (*), in which case the optimized small basis set (Sec. III C) is adopted. Note the decreasing IP values with increasing cluster sizes.

Model	Calculated IP (vertical transition)	Calculated NEXAFS transitions		
Isolated $NH_2(SiH_3)$	404.83*			
Isolated $NH_2(Si(SiH_3)_3)$	404.43*			
Isolated $NH_2(Si_9H_{12})$	404.10, 404.17*	*A*: 400.00	*B*: 400.80	*C*: 401.15
Zigzag ($Si_{15}H_{16}$)	403.99		*A*: 399.90	
H-bonded linear ($Si_{15}H_{16}$)	403.77 (H donor)		*A*: 399.85	
	404.17 (H acceptor)		*A*: 400.00	
H-bonded cross-trench ($Si_{33}H_{30}$)	403.30 (H donor)			
	403.98 (H acceptor)			

latter picture of ammonia adsorption at 300 K—in accord with the STM image interpretation of Refs. 10 and 11—can thus account for the experimental FWHM of the N 1*s* peak.

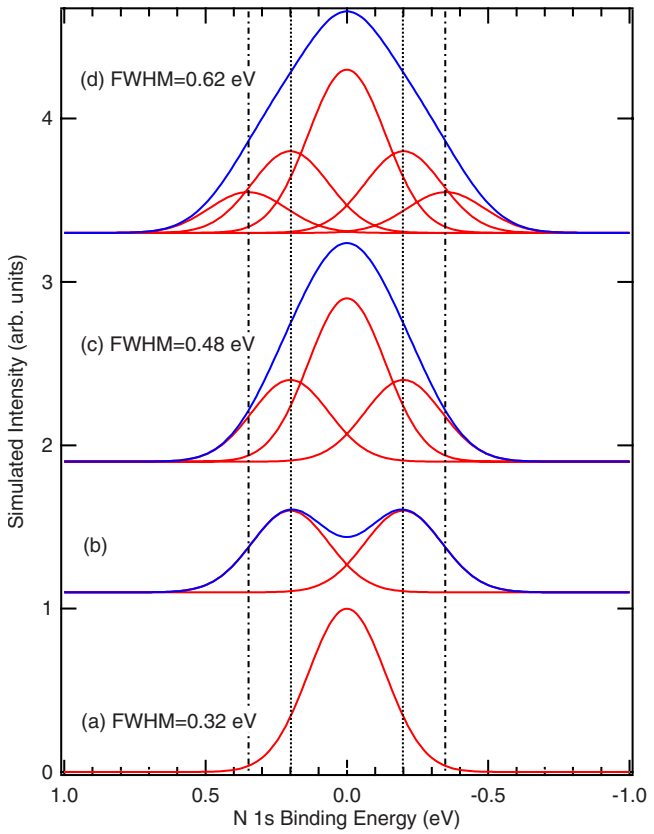

FIG. 6. (Color online) Synthetic N 1*s* curves considering (a) pure isolated amines, (b) pure intrarow linear patterns, (c) a 50:50 mixture of noninteracting amines and H bonded linear patterns, (d) a 40:40:20 mixture of noninteracting amines, H-bonded linear pattern, and cross-trench configurations. Each individual component is assimilated to a Gaussian of FWHM 0.32 eV (including vibrational, lifetime, and experimental broadenings). The overall FWHM of the synthetic curves is also given. The zero of binding energies is referenced to that of the isolated amine. In (d), we assume that the acceptor and donor IPs are symmetrical with respect to that of the isolated amine.

B. NEXAFS spectroscopy

The valence electronic structure of the $SiNH_2$ adduct is determined via N 1*s* NEXAFS spectroscopy that probes the empty molecular orbitals. The experimental spectra are given in Fig. 7. Concomitantly, useful information on the adsorbate bond orientation can be obtained by using highly anisotropic single-domain vicinal surface. The N 1*s* normalized absorption curves are measured with three orientations of the radiation polarization **E**: at 20° from the normal to the surface, parallel to the dimer axis, and parallel to the dimer rows (i.e., in plane, perpendicular to the dimer axis). From one acquisition scan to another, we have not noticed any change in the Auger yield curves, indicating that the sample degradation is insignificant. We indentify three absorption peaks positioned at photon energies 400.36 eV (*A*), 400.96 eV (*B*), and 401.64 eV (*C*). Despite the small photon bandwidth of 80 meV, we do not observe any vibrational fine structure. The relative intensities of peaks *A*, *B*, and *C* depend strongly on the orientation of **E**. Peak *B* is clearly associated to a UMO that has a strong *p* projection perpendicular to the surface plane. On the other hand, *A* and *C* peaks are transitions to UMOs having strong *p* projections within the surface plane. Here, the use of a single-domain vicinal surface is crucial: *A*(*C*) is stronger (weaker) when **E** is parallel to the dimer axis (parallel to the row direction). Therefore, the dichroic behavior of the N 1*s* spectrum indicates that the three absorption peaks at 400.36, 400.96, and 401.64 eV correspond to transitions to three UMOs with three *p* components born on orthogonal axes.

At this stage of the discussion, a comparison of the electronic structure of ammonia with that of the Si-NH_2 fragment is useful. Ammonia has three antibonding molecular orbitals: the lowest unoccupied molecular $4a_1^*$ (with the *p* component along the C_{3v} axis) and two degenerate $2e^*$ orbitals (with *p* components in a plane orthogonal to the C_{3v} axis). It is thus expected that substitution of a H atom by a Si atom to give the Si-NH_2 fragment will induce the splitting of the doubly degenerate $2e^*$ levels, hence the observation of three transitions in the N 1*s* NEXAFS spectrum of the ammonia covered surface. This expectation is confirmed by the Kohn-Sham contours of the antibonding orbitals of the NH_2 fragment to which one 1*s* electron is transferred (Fig. 8). For the sake of

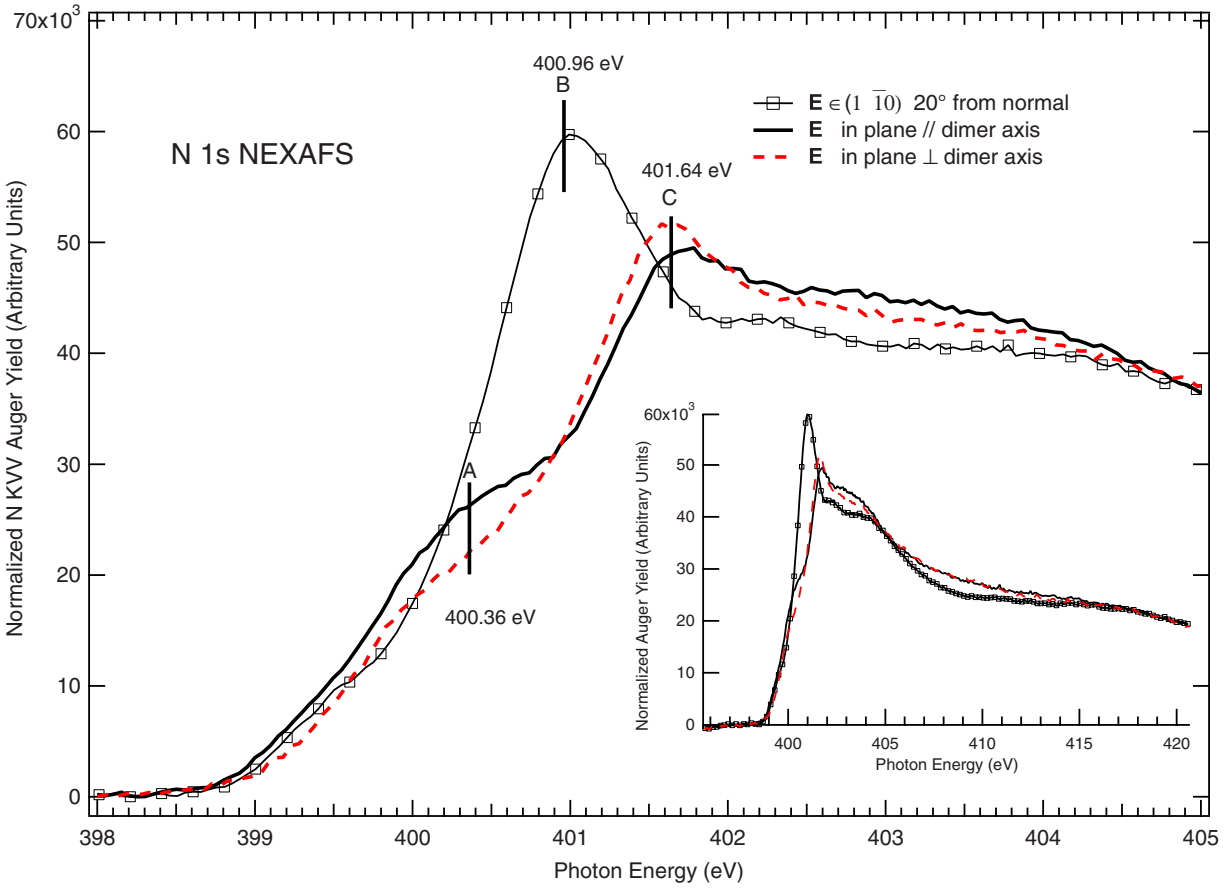

FIG. 7. (Color online) Normalized N 1*s* NEXAFS spectra of the single-domain Si(001)-2×1 surface exposed to ammonia under a pressure of 10^{-7} mbar for 15 min. The absorption curves are measured for three directions of the electric field **E**: 20° off the normal to the surface (continuous line and square markers), parallel to the Si-Si dimer axis (continuous black line), parallel to the dimer row (dashed black line). Note that transition *B* is polarized perpendicular to the surface plane, while transitions *A* and *C* are contained within the surface plane. Note also that *A* (c) is stronger (weaker) when **E** is parallel to the dimer axis (parallel to the row direction). Peak labeling is issued from core-excited-state DFT calculations (see also Fig. 8).

clarity, we show the case of the isolated anti $SiNH_2$ fragment attached to a Si_9H_{12} cluster. Orbital *A* derives clearly from the ammonia $4a_1^*$ orbital, while *B* and *C* are derived from the $2e^*$ one. The energies of the $(1s)^1(\text{UMO})^1$ states (referenced to the ground state) are also indicated in Fig. 8 (see also Table IV). They are in good quantitative agreement (to within ~0.3 eV) with the observed NEXAFS transitions of Fig. 7. Given this agreement, the common labeling of the experimental transitions and of the calculated antibonding molecular orbitals is justified. H bonding between intrarow pairs has also a limited effect on the molecular-orbital contours; the 1*s* to *A* ΔKS NEXAFS transitions energies is little affected ("acceptor" and "donor" transitions are split by only 0.15 eV, see Table IV), in contrast to what is observed for the IP. We have checked that the amine rotation around the Si-N axis does not modify appreciably the contours of the *A*, *B*, and *C* antibonding orbitals (apart from a change in the spatial orientation). Due to the fact that the Si-N axis makes an angle of about 21° with respect to the surface normal, it is clear from Fig. 8 that any rotation around this axis will let the "vertical" *p* component of UMO *B* little affected. On the other hand, the positioning of the NH_2 unit with respect to $[1\bar{1}0]$ and [110] axes can be easily determined from the in-plane dichroism of the two "horizontal" *p* components of *A* and *C* (that are orthogonal one to another). Naturally, the experimental implementation of this theoretical prediction could be made difficult by the co-occurrence of multiple adsorption patterns on the "real" surface.

To interpret the NEXAFS experimental data, we have calculated the theoretical absorption curves corresponding to the four intrarow models given in Fig. 1. The spectra simulated with a $(1s)^1(A)^1$ FCH-UMO potential are given in Fig. 9 The $(1s)^1(A)^1$ potential gives satisfactory energy spacing between the three adsorption structures $[E(B)\text{-}E(A) \sim 0.8$ eV, $E(C)\text{-}E(A) \sim 1.4$ eV] when compared to the ΔKS values reported in Table IV $[E(B)\text{-}E(A) \sim 0.8$ eV, $E(C)\text{-}E(A) \sim 1.2$ eV] and to the experimental values $[E(B)\text{-}E(A) \sim 0.6$ eV, $E(C)\text{-}E(A) \sim 1.3$ eV]. For all studied patterns, the intensity of peak *B* is maximum when the electric field **E** is perpendicular to the normal to the surface and is very weak when **E** is contained in the surface plane. As shown in Fig. 8, the *p* component of *B* is oriented rather normal to the surface and this orientation is not affected by the rotation of the amine around the Si-N axis. This is indeed observed experimentally. Spectrum simulations also show that peaks *A* and *C* are polarized within the surface plane.

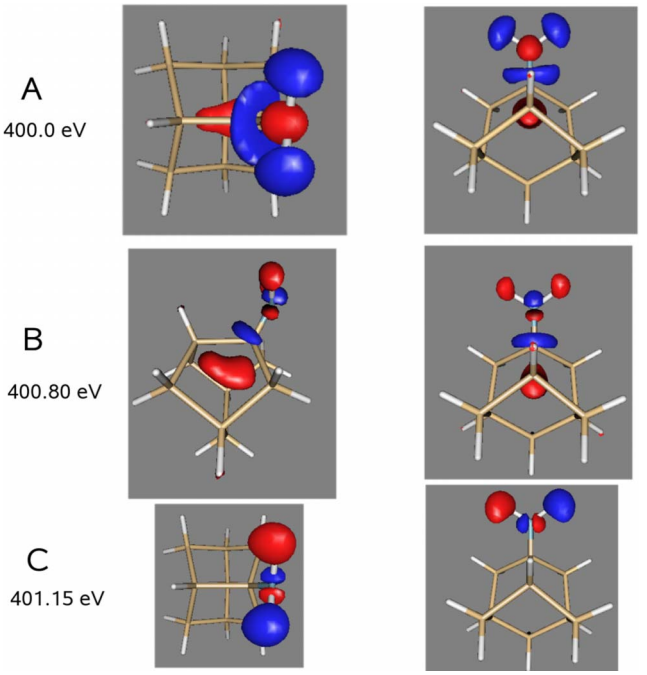

FIG. 8. (Color online) Contours of the unoccupied molecular orbitals $[(1s)^1(\mathrm{UMO})^1$ NEXAFS state] calculated for the isolated (anti)geometry of the Si-NH_2 fragment (a Si_9H_{12} cluster is used). The antibonding molecular orbitals *A*, *B*, and *C* are responsible for the most intense NEXAFS transitions with the same name in Fig. 7. The corresponding 1*s* to UMO ΔKS transition energies are also given.

Consequently, the various patterns are essentially distinguished one from another with the characteristic in-plane dichroism of structures *A* and *C*. The zigzag antipattern gives the most dichroic behavior with *A* strictly polarized along the Si-Si dimer axis and *C* along the dimer row (the dichroism can be easily guessed from the *p* component orientations of the three UMOs depicted in Fig. 8). The two gauche models give also dichroic in-plane absorption curves, but this time $A(C)$ is more intense when **E** is parallel to the dimer row (dimer axis). As expected from their respective orientations at right angle, the H-bonded amines of the linear pattern give practically nondichroic curves, for **E** parallel to the dimer axis and the dimer row

How do NEXAFS simulated spectra compare with experimental ones recorded at room temperature? Let us first examine the case of the pure linear pattern. The simulated NEXAFS spectra show a weak dichroism in the surface plane, in good accord with the experimental spectra. Note that the spectrum of the *cross-trench* H-bonded model we have not calculated should also be in good accord with the experiment, as its dichroic behavior should resemble that of the intrarow linear model [Fig. 9(d)], swapping the two in-plane directions. For their parts, none of the zigzag patterns provide, individually, the experimentally observed in-plane NEXAFS dichroism. The energies of the various zigzag patterns being quasidegenerate, their population should be nearly the same at 300 K, assuming low rotation barrier heights. The NEXAFS dichroism of the "averaged" zigzag patterns given in Fig. 10 agrees also satisfactorily with that of the experimental spectra.

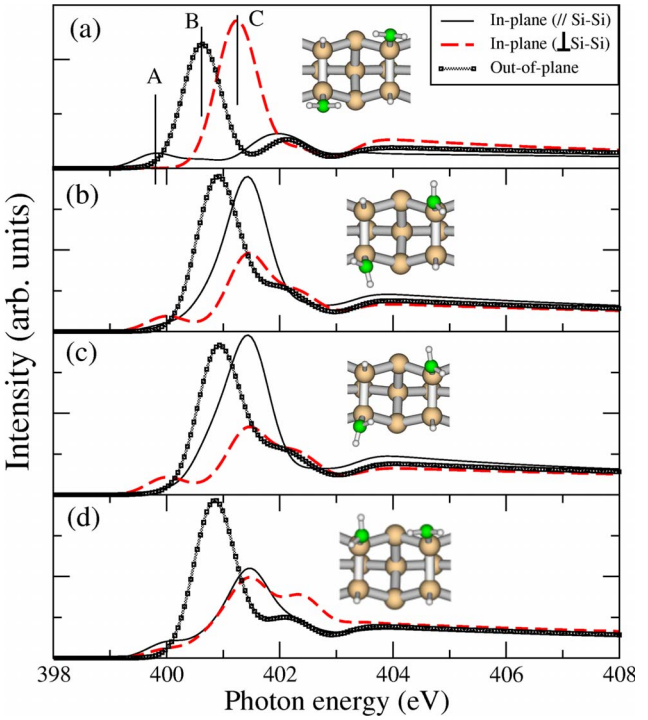

FIG. 9. (Color online) Theoretical NEXAFS spectra of NH_2 pairs relative to the adsorption patterns given in Fig. 1 along three directions: normal to the surface (squares), parallel to the Si-Si dimer axis (continuous black line), and parallel to the dimer row (dashed red line). A two-dimer $Si_{15}H_{16}$ cluster and a $(1s)^1(A)^1$ FCH-UMO potential are used. (a) The zigzag antipattern, (b) the zigzag gauche-C_2 pattern, (c) the zigzag gauche-*b* pattern, and (d) the linear (H-bonded pair) pattern.

V. CONCLUSIVE REMARKS

In this paper dedicated to the study of the electronic structure of a single-domain Si(001)-2×1 surface saturated by ammonia at 300 K, we present original N 1*s* XPS and NEXAFS data combined with hybrid functional DFT calculations of core-ionized/core-excited states. Despite the presence of bisteps, we have observed that the adsorption on vicinal surfaces leads to the exclusive dissociation of ammonia into H and NH_2 fragments, as it is the case for nominal (001) surfaces. The experimental N 1*s* XPS peak (binding energy 398.95 eV) measured with an experimental resolution of 80 meV is characterized by a symmetric and featureless shape (FWHM 675 meV). On the other hand, the simulated N 1*s* XPS spectral shape (taking into account the vibrational contribution) of the isolated amine is narrow (FWHM ~320 meV, taking an experimental resolution of 80 meV), asymmetric, and exhibits a clear ν(N-H) vibrational series. The discrepancy with experiment points to structural contributions to the observed N 1*s* XPS spectral broadening. The IP calculations confirm that H-bonding between amine pairs in intrarow linear patterns induces a N 1*s* binding-energy splitting of ~0.4 eV. This splitting increases to 0.7 eV for cross-trench H-bonding. IP splitting due to H bonding can be considered as a source of broadening in the XPS N 1*s* spectrum.

The empty molecular orbitals of the NH_2 fragment have been probed by N 1*s* NEXAFS spectroscopy. We have ob-

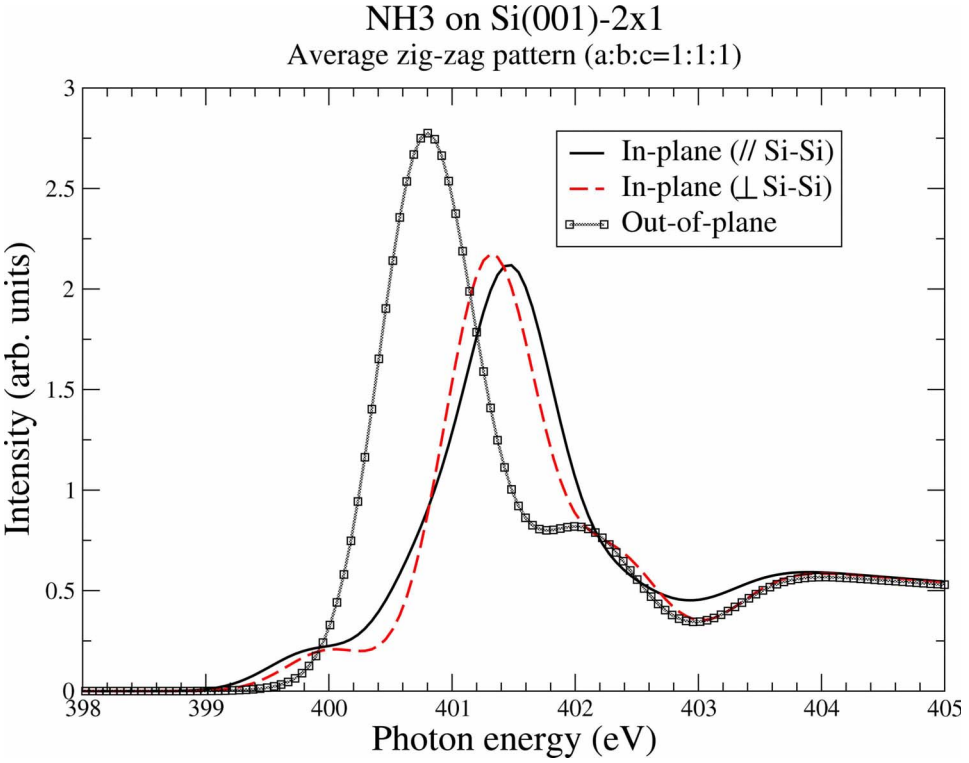

FIG. 10. (Color online) Theoretical NEXAFS spectra resulting from the sum of the three zigzag patterns curves [(a) anti, (b) gauche-C_2, and (c) gauche-C_1 of Fig. 8] with equal weights.

served three transitions at $h\nu$=400.36 eV (A), $h\nu$ =400.96 eV (B), and $h\nu$=401.64 eV (C). Calculated Δ Kohn-Sham transition energies of the ≡Si-NH_2 adduct are in very good agreement with the measured NEXAFS peak energies, which is a further confirmation of prior interpretations of the XPS N 1s spectra. The Kohn-Sham contours of the antibonding levels show that the rotation of the NH_2 fragment around the Si-N axis can be tracked by the dichroic behavior of NEXAFS transitions A and C within the (001) plane (B being always polarized perpendicular to the surface). The experimental N 1s absorption dichroism [within (001)] measured at 300 K can be satisfactorily reproduced by the simulated NEXAFS spectra of the H-bonded pattern and by the averaged contributions of the three nearly degenerate zigzag conformations.

The picture of the Si(001) surface dosed with ammonia at 300 K that emerges from this comparison between theory and experiment is that of mixed zigzag and linear patterns in comparable amounts (with inter-row interactions), in good accord with the interpretation of the STM occupied-state images of the saturated surface advocated by Bowler and Owen[10,11] and challenged by Chung and co-workers.[14–16] The calculated in-plane dichroic behavior of the N 1s NEXAFS curves suggests further experiments to be made. First, the linear-to-zigzag ratio could be modified by changing the adsorption temperature[11] [for instance, adsorption could be made below 120 K on a $c(4\times2)$ statically buckled surface[21]]. Second, in view of the application of the ammonia-reacted Si(001)-2×1 surfaces as templates for molecular layer deposition and supramolecular assembly, the present spectroscopic tools appear particularly well adapted to follow any change in the spatial orientation and chemical environment of the amine terminations in interaction with a molecular overlayer.

*Also at State Key Laboratory of Solidification Processing, Northwestern Polytechnical University, Xi'an 710072, People's Republic of China.
†Author to whom correspondence should be addressed. francois.rochet@upmc.fr

[1] M. Fujisawa, Y. Taguchi, Y. Kuwahara, M. Onchi, and M. Nishijima, Phys. Rev. B **39**, 12918 (1989).
[2] P. A. Taylor, R. M. Wallace, W. J. Choyke, M. J. Dresser, and J. T. Yates, Jr., Surf. Sci. **215**, L286 (1989).
[3] C. U. S. Larsson and A. S. Flodström, Surf. Sci. **241**, 353 (1991).
[4] C. U. S. Larsson, C. B. M. Andersson, N. P. Prince, and A. S. Flodström, Surf. Sci. **271**, 349 (1992).
[5] J. L. Bischoff, F. Lutz, D. Bolmont, and L. Kubler, Surf. Sci. **251-252**, 170 (1991).
[6] G. Dufour, F. Rochet, H. Roulet, and F. Sirotti, Surf. Sci. **304**, 33 (1994).
[7] K. T. Queeney, Y. J. Chabal, and K. Raghavachari, Phys. Rev. Lett. **86**, 1046 (2001).
[8] M. Z. Hossain, Y. Yamashita, K. Mukai, and J. Yoshinobu, Phys. Rev. B **68**, 235322 (2003).
[9] J. W. Kim and H. W. Yeom, Surf. Sci. **546**, L820 (2003).
[10] J. H. G. Owen, D. R. Bowler, S. Kusano, and K. Miki, Phys. Rev. B **72**, 113304 (2005).
[11] D. R. Bowler and J. H. G. Owen, Phys. Rev. B **75**, 155310 (2007).

[12] O. N. Chung, H. Kim, J.-Y. Koo, and S. Chung, Phys. Rev. B **74**, 193312 (2006).
[13] J. C. F. Rodriguez-Reyes and A. V. Teplyakov, Phys. Rev. B **76**, 075348 (2007).
[14] O. N. Chung, H. Kim, J.-Y. Koo, and S. Chung, Surf. Sci. Lett. **602**, L69 (2008).
[15] J. H. G. Owen and D. R. Bowler, Surf. Sci. **602**, 3760 (2008).
[16] J.-Y. Koo, H. Kim, O. N. Chung, and S. Chung, Surf. Sci. **602**, 3763 (2008).
[17] X. Cao and R. J. Hamers, J. Am. Chem. Soc. **123**, 10988 (2001).
[18] X. Cao, S. K. Coulter, M. D. Ellison, H. Liu, and R. J. Hamers, J. Phys. Chem. B **105**, 3759 (2001).
[19] M. Z. Hossain, S. Machida, Y. Yamashita, K. Mukai, and J. Yoshinobu, J. Am. Chem. Soc. **125**, 9252 (2003).
[20] M. Z. Hossain, S. Machida, Y. Yamashita, K. Mukai, and J. Yoshinobu, J. Phys. Chem. B **108**, 4737 (2004).
[21] J. Yoshinobu, Prog. Surf. Sci. **77**, 37 (2004).
[22] Y. Widjaja and C. B. Musgrave, J. Chem. Phys. **120**, 1555 (2004).
[23] G. M. Rignanese and A. Pasquarello, Appl. Phys. Lett. **76**, 553 (2000).
[24] G. M. Rignanese and A. Pasquarello, Surf. Sci. **490**, L614 (2001).
[25] S. Carniato, J.-J. Gallet, F. Rochet, G. Dufour, F. Bournel, S. Rangan, A. Verdini, and L. Floreano, Phys. Rev. B **76**, 085321 (2007).
[26] N. Franco, J. Avila, M. E. Davila, M. C. Asensio, D. P. Woodruff, O. Schaff, V. Fernandez, K.-M. Schindler, V. Fritzsche, and A. M. Bradshaw, Phys. Rev. Lett. **79**, 673 (1997).
[27] T. R. Leftwich and A. V. Teplyakov, Surf. Sci. Rep. **63**, 1 (2008).
[28] F. Rochet, F. Bournel, S. Carniato, G. Dufour, J.-J. Gallet, V. Ilakovac, K. L. Guen, S. Rangan, F. Sirotti, and S. Kubsky, Int. J. Nanosci. **6**, 85 (2007).
[29] We could think of isocyanates (to form a urea linkage), acyl chlorides/acid anhydrides (to form amides), ketones/aldehydes (to form imines), whose reaction with amines could be tested at room temperature and under low gas pressure (in the range 10^{-9}–10^{-7} mbar).
[30] J. C. F. Rodriguez-Reyes and A. V. Teplyakov, J. Phys. Chem. C **111**, 16498 (2007).
[31] J. Gardener, J. H. G. Owen, K. Miki, and S. Heutz, Surf. Sci. **602**, 843 (2008).
[32] J. Stöhr, *NEXAFS Spectroscopy*, Springer Series in Surface Sciences (Springer-Verlag, Berlin, 1992).
[33] http://www.synchrotron-soleil.fr/portal/page/portal/Recherche/LignesLumiere/TEMPO
[34] With a miscut angle α, the average number of Si_2 dimers in a row on a terrace, is $n_{\text{dimer}}^{\text{terrace}} = \frac{1}{\sqrt{2}\times\tan\alpha} - \frac{1}{2}$.
[35] M. Dürr, Z. Hu, A. Biedermann, U. Höfer, and T. F. Heinz, Phys. Rev. B **63**, 121315(R) (2001).
[36] http://www.msg.ameslab.gov/GAMESS/GAMESS.html
[37] A. Becke, J. Chem. Phys. **98**, 5648 (1993).
[38] C. Lee, W. Yang, and R. G. Parr, Phys. Rev. B **37**, 785 (1988).
[39] X. Xu and W. A. Goddard III, Proc. Natl. Acad. Sci. U.S.A. **101**, 2673 (2004).
[40] T. Todorova, A. P. Seitsonen, J. Hutter, I.-F. W. Kuo, and C. J. Mundy, J. Phys. Chem. B **110**, 3685 (2006).
[41] J.-H. Cho and K. S. Kim, Phys. Rev. B **62**, 1607 (2000).
[42] S. Rangan, F. Bournel, J.-J. Gallet, S. Kubsky, K. Le Guen, G. Dufour, F. Rochet, F. Sirotti, S. Carniato, and V. Ilakovac, Phys. Rev. B **71**, 165319 (2005).
[43] S. Carniato, F. Rochet, J.-J. Gallet, F. Bournel, G. Dufour, and C. Mathieu, Surf. Sci. **601**, 5515 (2007).
[44] S. Carniato, V. Ilakovac, J.-J. Gallet, E. Kukk, and Y. Luo, Phys. Rev. A **71**, 022511 (2005).
[45] L. Triguero, J. Electron Spectrosc. Relat. Phenom. **104**, 195 (1999).
[46] T. Ziegler, A. Rauk, and E. J. Baerends, Theor. Chim. Acta **43**, 261 (1977).
[47] P. W. Langhoff, Chem. Phys. Lett. **22**, 60 (1973).
[48] The computation of the energy Hessian included in the GAMESS package (Ref. 36 of the present paper) permits the prediction of vibrational frequencies.
[49] S. Carniato, J. Chem. Phys. **126**, 224307 (2007).
[50] S. Carniato and P. Millié, J. Chem. Phys. **116**, 3521 (2002).
[51] S. Carniato and Y. Luo, J. Electron Spectrosc. Relat. Phenom. **142**, 163 (2005).
[52] F. J. Himpsel, B. S. Meyerson, F. R. McFeely, J. F. Morar, A. Taleb-Ibrahimi, and J. A. Yarmoff, in *Core Level Spectroscopy at Silicon Surfaces and Interfaces*, Proceedings of the International School of Physics "Enrico Fermi," Course CVIII, Varenna, (1988) Vol. 222, edited by M. Campagna and R. Rosei (North-Holland, Amsterdam, 1990).
[53] K. C. Prince, M. Vondráček, J. Karvonen, M. Coreno, R. Camilloni, L. Avaldi, and M. de Simone, J. Electron Spectrosc. Relat. Phenom. **101-103**, 141 (1999).
[54] Changes in the calculated IP can be viewed as "final-state" effects: the relaxation energy, i.e. the ability of the system to screen out the nitrogen core hole, increases with the silicon cluster size. On the other hand, Mulliken charges in the *ground state* do not vary much with increasing the silicon cluster size [they amount to −0.71, −0.73 and −0.71 unit charge for SiH_3, $Si(SiH_3)_3$, and Si_9H_{12}, respectively].
[55] As the calculation of the vibrational fine structure of the N 1*s* spectrum of paired amines was largely beyond the scope of the present paper, we have assumed here that we can sum two, split apart, components having the same width as that calculated for an isolated amine. As a matter of facts, the H bond between two amines is relatively weak (the N-N distance is in the range 3.3–3.55 Å). Stronger H bonds may have non-negligible effects on component widths. Indeed in the case of the water dimer (O-O distance of 2.91 Å, see Ref. 25), the hydrogen bonding and the drastic change in water-dimer potential under O 1*s* core ionization are responsible for an anomalously strong vibrational broadening of both the donor and acceptor oxygens. See V. C. Felicíssimo, I. Minkov, F. F. Guimaraes, F. Gel'mukhanov, A. Cesar, and H. Ågren, Chem. Phys. **312**, 311 (2005).